

System Identification and Cable Force Control for a Cable-Driven Parallel Robot with Industrial Servo Drives

Werner Kraus, Valentin Schmidt, Puneeth Rajendra and Andreas Pott

Abstract—In a cable-driven parallel robot, elastic cables are used to manipulate the end effector in the workspace. In this paper we present a dynamic analysis and system identification for the complete actuator unit of a cable robot including servo controller, winch, cable, cable force sensor and field bus communication. We establish a second-order system with dead time as an analogous model. Based on this investigation, we propose the design and stability analysis of a cable force controller. We present the implementation of feed-forward and integral controllers based on a stiffness model of the cables. As the platform position is not observable the challenge is to control the cable force while maintaining the positional accuracy. Experimental evaluation of the force controller shows, that the absolute positional accuracy is even improved.

I. INTRODUCTION

Due to their huge workspace, high dynamics and lightweight structure, cable-driven parallel robots, in the following referred to as cable robots, received high interest in the past. For stable operation of the robot, all the cables have to be kept under tension. This can be achieved using the criterion of the wrench-feasible workspace, which includes all positions where the platform can be held in static equilibrium using positive bounds on cable forces [1]. The workspace determination for cable robots is the topic of many publications, e.g. in [1], [2], [3] and [4]. To exploit the numerically computed workspace on the real robot, one has to control the cable forces. Especially for cable robots with more cables than degrees of freedom this becomes relevant due to infinite solutions for the cable forces. Beside a bigger usable workspace this can also lead to interesting strategies to reduce the energy consumption or to reach high stiffness of the robot.

Many publications address the determination of feasible force distributions for cable robots, e.g. in [5], [6]. For the use in control purposes, the algorithms must deliver continuous solutions for the cable forces and fulfill the real-time constraint [7], [8], [9].

The dynamic control of classical parallel kinematic machines were discussed in [10] and [11]. Known challenges are the non-linear dynamic and the unobservable position and orientation of the end effector. Also for cable robots, direct torque control approaches are proposed in [12]. Control approaches with simulation are shown in [13] and [14]. An extensive work on the control of a cable-driven locomotion interface can be found in [15]. There exist several paper

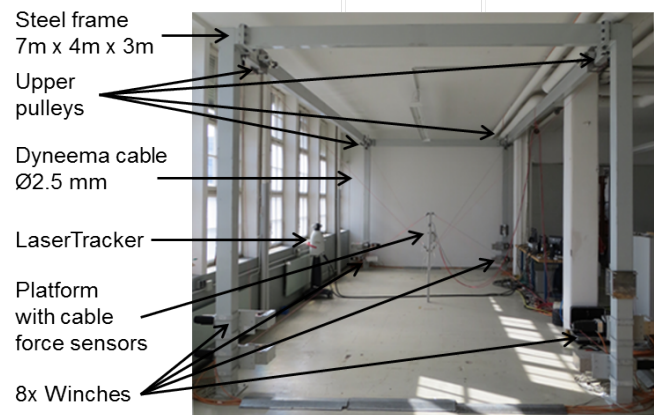


Fig. 1. Cable-driven parallel robot IPAnema 2

on the implementation of controller for cable robots with practical evaluation [16], [17], [18], [19], [20].

This paper focuses on the system identification and cable force control of a cable robot using industrial servo drives and control technology. Reasons for using industrial hardware are customer acceptance, availability of the products and stability. One requirement for the operation of a cable robot is a deterministic and synchronous control of each winch. This is fulfilled by a real-time field bus. The position controller of the servo amplifier can only be parametrized, but not modified as they are industrial grade components. Also the motion kernel of the Computerized Numerical Control (CNC) with trajectory generator and interpolator largely restricts extensions of the control algorithms. Therefore, we implement the control algorithm on the Programmable Logic Controller (PLC), which runs in real-time synchronous to the CNC.

The cable force control faces several challenges. Some of them we already investigated in the past:

- 1) Through the force and torque equilibrium at the platform, the cable forces influence the position and orientation of the platform. [21]
- 2) The pose of the platform cannot be measured. Spatial closed-loop Cartesian position control is not feasible for lack of measuring equipment. [10],
- 3) The cable forces influence each other at the platform. [21]
- 4) The cable force measurement is influenced by uncertainties in the force sensors and geometrical parameters of the robot [21]

This work was supported as a Fraunhofer Master Project.

All the authors are with the Fraunhofer Institute for Manufacturing Engineering and Automation IPA in Stuttgart, Germany
 Werner.Kraus at ipa.fhg.de

From point 2 follows we cannot implement a closed loop position control which is superordinated regarding the cable force controller. Therefore, we cannot compensate for positional deviation caused by the force controller. Points 3 and 4 deliver that the cable force controllers will never reach a control error of 0. Unlimited integral controllers for cable forces will lead to positional errors because of point 1. To remain the positional accuracy, we have to limit the influence of the cable force controller on the cable length. These points lead to proposed control algorithm.

This paper is organized as follows: In Section II we briefly recall the theoretical foundations for the robot kinematics, dynamics, and the determination of feasible force distributions. Next, the system identification for a single winch is discussed. Based on the analogous model of the system, we present the controller design and implementation on the robot controller in Section IV. Finally, experimental results regarding control and positional accuracy are presented.

II. ROBOT MODEL

For completeness, we briefly review the robot model. The geometry of the robot is described by proximal anchor points on the robot base A_i and the distal anchor points on the end effector B_i . The index i denotes the cable number and m is the absolute number of cables. By applying a vector loop as shown in figure 2 the cable vector \mathbf{l}_i follows as

$$\mathbf{l}_i = \mathbf{a}_i(\mathbf{r}, \mathbf{R}) - \mathbf{r} - \mathbf{R} \mathbf{b}_i, \quad (1)$$

while \mathbf{r} is the platform position vector and rotation matrix \mathbf{R} describes the platform orientation. As we take the pulleys at winches into account, the vector \mathbf{a}_i to the starting point of the cable depends on the current pose of the robot [22].

The structure equation with the structure matrix \mathbf{A}^T resulting from the force and torque equilibrium at the end effector for the cable force distribution \mathbf{f} is given by

$$\underbrace{\begin{bmatrix} \mathbf{u}_1 & \cdots & \mathbf{u}_m \\ \mathbf{b}_1 \times \mathbf{u}_1 & \cdots & \mathbf{b}_m \times \mathbf{u}_m \end{bmatrix}}_{\mathbf{A}^T(\mathbf{r}, \mathbf{R})} \underbrace{\begin{bmatrix} f_1 \\ \vdots \\ f_m \end{bmatrix}}_{\mathbf{f}} = - \underbrace{\begin{bmatrix} \mathbf{f}_p \\ \boldsymbol{\tau}_p \end{bmatrix}}_{\mathbf{w}}, \quad (2)$$

where $\mathbf{u}_i = \frac{\mathbf{l}_i}{\|\mathbf{l}_i\|}$. The wrench \mathbf{w} consists of external forces \mathbf{f}_p and torques $\boldsymbol{\tau}_p$ and includes also the gravity g .

The dynamic wrench on the platform for a given translational and rotational acceleration \mathbf{a} and $\boldsymbol{\alpha}$ and rotational velocity $\boldsymbol{\omega}$ can be described as follows

$$\begin{bmatrix} \mathbf{f}_{\text{dyn}} \\ \boldsymbol{\tau}_{\text{dyn}} \end{bmatrix} = \begin{bmatrix} m_p \mathbf{I} & -m_p [\mathbf{c}] \\ m_p [\mathbf{c}] & \mathbf{J}_c - m_p [\mathbf{c}][\mathbf{c}] \end{bmatrix} \begin{bmatrix} \mathbf{a} \\ \boldsymbol{\alpha} \end{bmatrix} + \begin{bmatrix} m_p \boldsymbol{\omega} \times (\boldsymbol{\omega} \times \mathbf{c}) \\ \boldsymbol{\omega} \times (\mathbf{J}_c - m_p [\mathbf{c}][\mathbf{c}]) \boldsymbol{\omega} \end{bmatrix}, \quad (3)$$

where m_p is the mass of the platform, \mathbf{J}_c is the inertia tensor respect to the center of mass \mathbf{c} and $[\mathbf{c}]$ the skew-symmetric matrix, for which an arbitrary vector \mathbf{a} holds $[\mathbf{c}]\mathbf{a} = \mathbf{c} \times \mathbf{a}$.

To compute a force distribution \mathbf{f} , which solves the structure equation (2) and is continuous along a trajectory,

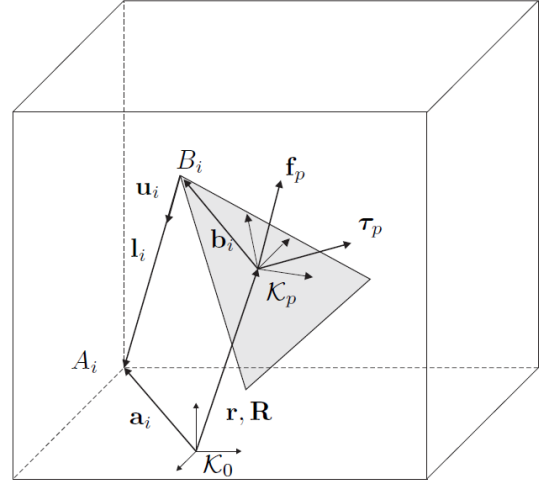


Fig. 2. Robot kinematic

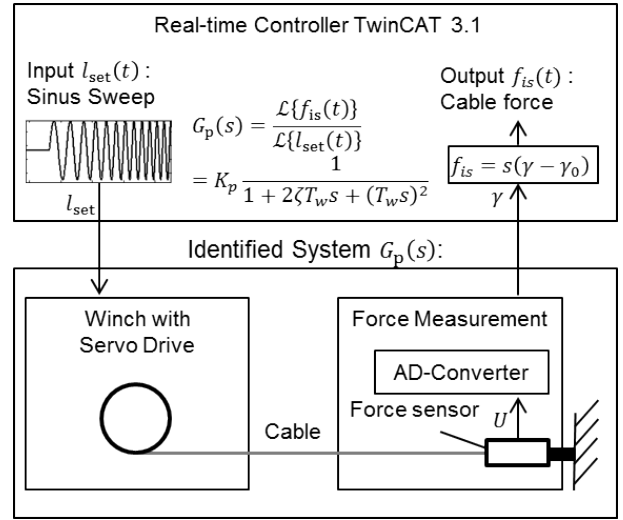


Fig. 3. Experimental system identification for one winch with servo drive and force measurement

the closed-form solution presented in [23] is used. In this approach, a medium feasible force distribution $\mathbf{f}_m = (\mathbf{f}_{\min} + \mathbf{f}_{\max})/2$ is introduced which is based on the minimum f_{\min} and maximum cable force f_{\max} , respectively. With the Moore-Penrose matrix inverse \mathbf{A}^{+T} the force distribution is obtained by

$$\mathbf{f} = \mathbf{f}_m - \mathbf{A}^{+T}(\mathbf{w} + \mathbf{A}^T \mathbf{f}_m). \quad (4)$$

Hint: Principally, the presented control approach is compatible with every method which solves the structure equation (2).

III. SYSTEM IDENTIFICATION

In the first step, we investigate the dynamic behaviour of one servo winch including servo controller, cable and force measurement by setting position trajectories and measuring the corresponding cable force. This allows for identifying the parameters of an analogous model.

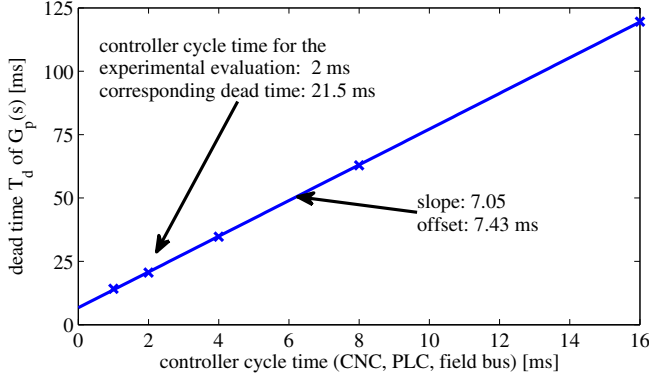


Fig. 4. Correlation between dead time T_d of the plant $G_p(s)$ and controller cycle time T_c

For system identification, a single winch is investigated by connecting the cable to a fixed point. The structure of the identified system is shown in figure 3. A sinusoidal oscillation with variable frequency from 1 to 20 Hz for the cable length is generated in the PLC and commanded via the field bus to the servo amplifier. There, the cascaded position controller with the closed feedback loop over the motor encoder sets the commanded cable length and tensions the cable. The signal from the cable force sensor is digitized and sent back to the PLC via the field bus.

We perform the identification experiment with different cycle times T_c of the controller and field bus in the range of 1 to 16 ms and analyze the dead time T_d between commanded cable length and resulting force. There is a linear correlation between cycle time and dead time, as shown in figure 4. The reason for the dead time is that the signal passes several layers of communication in discrete time steps, e.g. from the CNC to the field bus. This is represented in the slope, which reveals that the dead time rises seven time faster than the cycle time. The offset of 7.43 ms (at cycle time of 0) is mainly caused by the conversion time of the A/D-converter. The investigated system is a typical spring-mass-damper-system with time-discrete control. Therefore, we assume a second order system with dead time

$$G_p(s) = K_p \frac{1}{1 + 2\zeta T_w s + (T_w s)^2} e^{-T_d s} \quad (5)$$

for the transmission behavior from set cable length l_{set} to measured cable force f_{is} . For the parameter identification of the transfer function we use the Matlab System Identification Toolbox. The resulting parameters are listed in table I. The measurement is reflected with a goodness fit of 83.92% by the identified transfer function. The deviation of 16% mainly arises from sensor noise which is not modeled.

The Bode diagram for the controller cycle time T_c of 2 ms is shown in figure 5. The magnitude curve is relatively uniform with a small peak at the eigenfrequency at about 12 Hz. The phase curve is plotted for the complete system $G_p(s)$ and splitted up in the system dynamic

$$G_{p,1}(s) = K_p \frac{1}{1 + 2\zeta T_w s + (T_w s)^2} \quad (6)$$

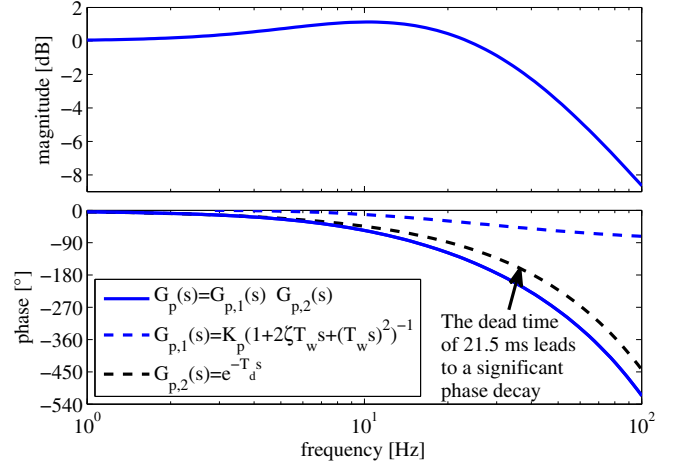


Fig. 5. Bode diagram of the identified system $G_p(s)$ consisting of servo drive, cable, force sensor with A/D-converter and communication at a controller cycle time T_c of 2 ms

TABLE I
IDENTIFIED PARAMETERS AND CONTROL PARAMETERS

parameter	definition	value	unit
K_p	proportional gain, depends on cable length	k_0/l_i	N/m
ζ	damping ratio	0.5100	-
T_w	natural period	0.0048	rad/s
T_d	dead time	0.0215	s
T_i	integrator reset time	0.2	s
T_1	PT ₁ time constant	0.02	s
T_c	controller cycle time	2	ms
ΔF_{sat}	saturation of the integrator	± 80	N
k_0	specific cable stiffness	120	kN

and the influence of the dead time

$$G_{p,2}(s) = e^{-T_d s} \quad (7)$$

The phase curve reveals a strong decay due to the dead time of 21.5 ms. The contribution of the remaining system dynamic is relatively small.

IV. CONTROLLER DESIGN AND IMPLEMENTATION

The force controller has to deal with a couple of challenges. As we can only add changes in cable length to the drives, we need a transformation between cable forces to cable elongation over a stiffness model of the cables. The cable characteristic can only be estimated, as it is time-variant and influenced by settlement and creeping. As already discussed in [24], the force sensors are subject to fluctuations regarding their characteristics. Another problem is the dead time of the control loop, which leads to instabilities.

For the overall control, we have to find a compromise between positional accuracy of the end effector and force control deviation. The analytically derived cable force distribution is afflicted by a series of model uncertainties like geometry of the robot and the assumption that the end effector is at the desired pose. Furthermore, all single controllers interact continuously with each other. Due to the mentioned influences, the calculated cable force distribution does not

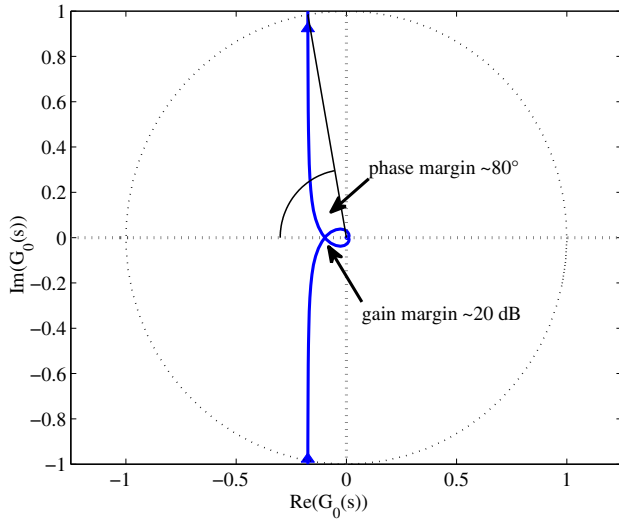


Fig. 6. Nyquist diagram for the open loop transfer function $G_0(s)$

exist on the real robot and therefore we cannot reach static accuracy for the force control.

To deal with these challenges, we propose a model-based feed-forward control and an integral control with anti-windup. The idea of the feed-forward-control is, to tension the cable according to the stiffness model neglecting the feedback value. It allows for fast adaption to changing setpoint values and improves the system response and stability.

In the initial configuration of the robot, the cables are already under tension to stabilize the platform. This pretension has to be taken into account for the feed-forward-control. Therefore, we subtract the initial cable forces $\mathbf{f}_{\text{initial}}$ from the desired cable forces \mathbf{f}_{set}

$$\mathbf{f}_{\text{ff}} = (\mathbf{f}_{\text{set}} - \mathbf{f}_{\text{initial}}) \quad (8)$$

and receive the feed-forward control term \mathbf{f}_{ff} . It is directly added to the controller output $\mathbf{f}_{\text{c,out}}$.

In the feedback loop $G_r(s)$ we introduce a PT_1 -filter

$$G_r(s) = \frac{1}{1 + T_1 s} \quad (9)$$

with time constant T_1 to reduce the influence of sensor noise. We apply an integral controller $G_c(s)$

$$G_c(s) = \frac{1}{T_i s} \quad (10)$$

where T_i is the integrator reset time. As we cannot reach static accuracy in the cable forces, the maximum controller output is limited by ΔF_{sat} . To avoid saturation of the integrator, an anti-windup is implemented.

The controller output $\mathbf{f}_{\text{c,out}}$ which consists of the integral controller with saturation and the feed-forward controller is transformed with the stiffness estimation $C = k_0/l_i$ of the cables based on the specific stiffness constant k_0 and their actual cable lengths l_i with

$$\Delta l = \mathbf{f}_{\text{c,out}} C \quad (11)$$

into the change in cable length Δl .

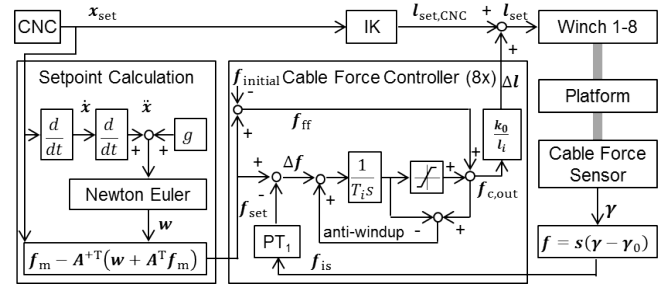


Fig. 7. Controller implementation on the PLC

The dead time in the transfer function $G_p(s)$ described in equation (5) leads to a transcendental transfer function, which cannot be handled by control design algorithms. Therefore, we transform the dead time to an allpass with a Padé approximation

$$e^{-T_d s} \approx \tilde{G}_{p,2}(s) = \frac{1 - \frac{T_d s}{2} + \frac{(T_d s)^2}{12}}{1 + \frac{T_d s}{2} + \frac{(T_d s)^2}{12}} \quad (12)$$

of second order and establish the transfer function $\tilde{G}_p(s) \approx G_{p,1}(s)\tilde{G}_{p,2}(s)$. The stability of the control can now be evaluated with the open loop transfer function $G_0(s)$

$$G_0(s) = G_c(s)\tilde{G}_p(s)G_r(s) \quad (13)$$

whose Nyquist diagram with the stability margins is shown in figure 6. The controller is parametrized regarding a high stability with conservative gain and phase margin of 20 dB and 80° , respectively. The conservative parametrization is necessary to avoid oscillations due to the interaction of eight individual integral controllers.

The controller is implemented on a real-time PLC according to figure 7. The existing CNC with the Inverse Kinematic (IK) which sets cable lengths to the winches is appended with change in cable length Δl . The force sensor in each cable and the calibration parameters s and γ_0 provide the actual force distribution \mathbf{f}_{is} to the controller.

In the setpoint calculation module, the dynamic wrench is determined for the commanded acceleration with equation (3). Next, a feasible force distribution \mathbf{f}_{set} is evaluated for the commanded position according to equation (4).

The robot control is realized on an industrial PC with Beckhoff TwinCAT 3.1 CNC at a cycle time of 2 ms. The field bus protocol is SERCOS 2. For the force measurement the robot is equipped with eight cable force sensors (meas-spec, XFTC-300-A1-2.000) at the end effector. The sensors have a resolution of 0.13 N and a measurement range of ± 2000 N. The analog output signal of the force sensors is digitized in A/D-converters and sent via the field bus to the control. The cable type is LIROS D-Pro 01505-0250 based on Dyneema SK 75 fibre (Polyethylene) with a diameter of 2.5 mm.

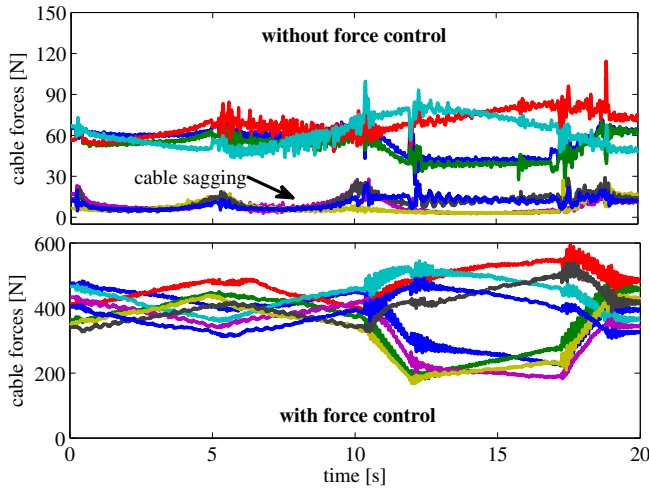


Fig. 8. Cable forces without (top) and with (bottom) force control

V. EXPERIMENTAL EVALUATION

In the following, we discuss the experimental evaluation of the cable force controller regarding its control and positional accuracy. The experiments are performed on the IPAnema 2 shown in figure 1.

The effect of the force control on the cable forces can be seen in figure 8. Without force control (just position control with the inverse kinematic) certain cables are temporally not tensed and tend to sag, whereas the same remains in tension due to force control.

Performance evaluations of the controller are presented in table II. The experiment is conducted by varying the position by 0.2m in z axis for every measurement. Due to model uncertainties and sensor noise the controller cannot reach the perfect static accuracy. The data reveal, that the absolute mean control error for the cable forces ranges between 5 and 18 N, whereas the maximum error goes up to 68 N for one certain position.

To investigate the following behaviour of the force control, the robot was programmed to follow a 3 m long path at velocities ranging from 0.5 to 2.0 m/s. The control errors rise with the velocity, as can be seen quantitatively in table II. For the reason of clearness, in figure 9 only for one cable the measured f_{is} and setpoint force f_{set} and their difference df is shown. The diagram reveals qualitatively the rising control error at higher velocities. As the platform is mainly position controlled, the error in force control is still acceptable and does not lead to instabilities of the robot.

The transition phase activating the force controls leads to some interesting observations. We see that initially the cable force is around 120 N, enabling the feed-forward control rises the cable force in the range of the desired value. One can see a decrease of the force within 1 second, which is the result of the cable settling on the drum. Enabling the feedback loop leads to a transition of the cable forces near the setpoint value.

TABLE II
EXPERIMENTAL RESULTS FOR THE CONTROL ERROR OF THE FORCE CONTROLLER

scenario	absolut mean error [N]	maximum error [N]
static		
[+0.75 +0.5 +0.2 → +1.0]	12.467	44.658
[+0.75 -0.5 +0.2 → +1.0]	5.574	25.735
[-0.75 -0.5 +0.2 → +1.0]	8.309	38.921
[+1.50 +1.0 +0.2 → +1.0]	17.306	67.809
[+1.50 -1.0 +0.2 → +1.0]	6.426	28.686
[-1.50 -1.0 +0.2 → +1.0]	7.844	42.202
dynamic		
3 m long path with 0.5 m/s	8.366	35.612
3 m long path with 1.0 m/s	11.086	44.284
3 m long path with 1.5 m/s	11.731	49.103
3 m long path with 2.0 m/s	12.847	52.464

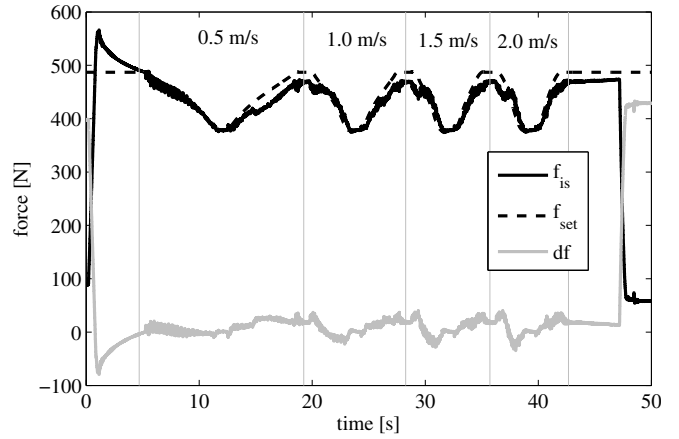


Fig. 9. Force in one cable during a trajectory with different velocities up to 2.0 m/s

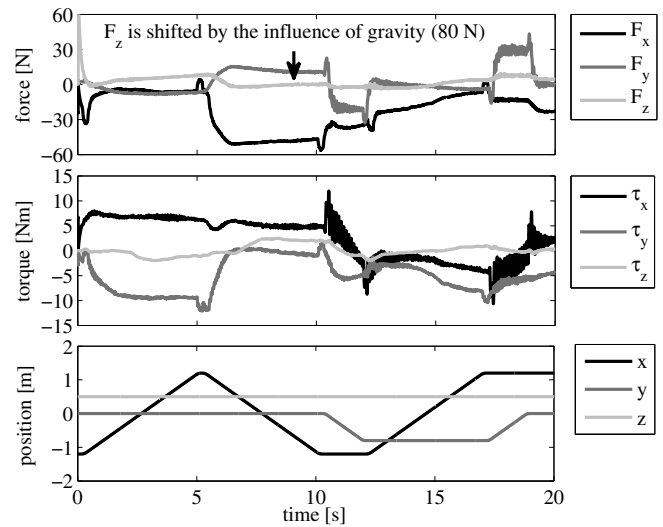


Fig. 10. Course of the wrench based on the measured cable forces on a rectangular trajectory

TABLE III

EXPERIMENTAL RESULTS FOR THE ABSOLUTE POSITIONING ACCURACY
IN [MM] WITHOUT AND WITH FORCE CONTROL

pose	without force control	with force control
[+0.75 +0.5 +0.2 → +1.0]	42.22	38.14
[+0.75 -0.5 +0.2 → +1.0]	54.87	39.74
[-0.75 -0.5 +0.2 → +1.0]	33.83	16.81
[+1.50 +1.0 +0.2 → +1.0]	46.79	46.00
[+1.50 -1.0 +0.2 → +1.0]	71.38	53.89
[-1.50 -1.0 +0.2 → +1.0]	23.76	9.83
average	45.48	34.07

Figure 10 shows the course of the wrench w , which is determined with the measured cable forces according to equation (2). Obviously, the acceleration and deceleration leads to peaks in the force. Furthermore, the diagram reveals, that the measured wrench changes over the trajectory although the weight of the platform does not change. This effect is due to the mentioned uncertainties.

The positional accuracy of the robot is measured with an absolute LaserTracker. As shown in table III, the mean of the errors in all Cartesian directions are tabulated with and without force control, which indicates an improvement in the absolute positional error. The overall average error for the tested workspace is comparatively better with force control. In [24] we investigated the relative positional accuracy of the IPAnema under changing loads and received values less than 1 mm. The present findings are worse because they are absolute regarding the robot coordinate system.

VI. CONCLUSION

Using a system identification, we established a second order system with dead time as an analogous model for the actuator unit of a cable robot with industrial servo drives. The dynamic of the control loop depends significantly on the cycle time of the controller. Doubling the cycle time leads to an increase of the system dead time by factor 7. Based on the identified analogous model, we developed and implemented a cable force controller. The performance regarding control accuracy, stability and positional accuracy was demonstrated on the cable robot IPAnema 2.

Further investigation could focus on the power consumption of the robot and strategies to improve the energy efficiency. The cable force control could also be extended to a Cartesian control which can control the contact forces between the robot and environment. Based on the analogous model, other control strategies like impedance control could be developed.

REFERENCES

- [1] R. Verhoeven, "Analysis of the workspace of tendon-based Stewart platforms," Ph.D. dissertation, University of Duisburg-Essen, Duisburg, 2004.
- [2] S. Bouchard, C. M. Gosselin, and B. Moore, "On the ability of a cable-driven robot to generate a prescribed set of wrenches," in *Journal of Mechanisms and Robotics*, vol. 2, no. 1, 2010, pp. 1–10.
- [3] M. Hassan and A. Khajepour, "Analysis of bounded cable tensions in cable-actuated parallel manipulators," in *IEEE Transactions On Robotics*, vol. 27, 2011, pp. 891–900.

- [4] M. Gouttefarde, D. Daney, and J. P. Merlet, "Interval-analysis-based determination of the wrench-feasible workspace of parallel cable-driven robots," in *IEEE Transactions On Robotics*, vol. 27, no. 1, 2011, pp. 1–13.
- [5] H. D. Taghirad and Y. B. Bedoustani, "An analytic-iterative redundancy resolution scheme for cable-driven redundant parallel manipulators," in *IEEE Transactions On Robotics*, 2011, pp. 1–7.
- [6] P. H. Borgstrom, B. L. Jordan, G. S. Sukhatme, M. A. Batalin, and W. J. Kaiser, "Rapid computation of optimally safe tension distributions for parallel cable-driven robots," in *IEEE Transactions On Robotics*, vol. 25, no. 6, 2009, pp. 1271–1281.
- [7] J. Lamaury and M. Gouttefarde, "A tension distribution method with improved computational efficiency," in *Cable-Driven parallel robots*. Springer Berlin Heidelberg, 2013, pp. 71–85.
- [8] A. Pott, "An improved Force Distribution Algorithm for Over-Constrained Cable-Driven Parallel Robots," in *Computational Kinematics 2013*, Frederico Thomas and Alba Pérez Gracia, Eds., 2013.
- [9] K. Yu, L. Lee, V. Krovi, and C. Tang, "Enhanced trajectory tracking control with active lower bounded stiffness control for cable robot," in *IEEE International Conference on Robotics and Automation*, 2010, pp. 669–674.
- [10] F. Paccot, N. Andreff, and P. Martinet, "A review on the dynamic control of parallel kinematic machines: Theory and experiments," in *International Journal of Robotic Research*, vol. 28, no. 3. Thousand Oaks, CA, USA: Sage Publications, Inc., Mar. 2009, pp. 395–416.
- [11] J. Wang, J. Wu, L. Wang, and Z. You, "Dynamic feed-forward control of a parallel kinematic machine," in *Mechatronics*, vol. 19, no. 3. Springer Netherlands, 2009, pp. 313 – 324.
- [12] X. Liu, Y. Qiu, and X. Duan, "Stiffness enhancement and motion control of a 6-dof wire-driven parallel manipulator with redundant actuations for wind tunnels," in *Intechopen*, 2009.
- [13] G. Meunier, B. Boulet, and M. Nahon, "Control of an overactuated cable-driven parallel mechanism for a radio telescope application," *IEEE Transactions on Control Systems Technology*, vol. 17, no. 5, pp. 1043–1054, 2009.
- [14] E. Laroche, R. Chellal, L. Cuvillon, and J. Gangloff, "A Preliminary Study for H_∞ Control of Parallel Cable-Driven Manipulators," in *Mechanisms and Machine Science*. Springer Berlin Heidelberg, 2013, pp. 353–369.
- [15] M. J.-D. Otis, T.-L. Nguyen Dang, Laliberte Thiery, D. Quellet, D. Laurendeau, and C. Gosselin, "Cable Tension Control and Analysis of Reel Transparency for 6-DOF haptic foot platform on a cable-driven locomotion interface," in *International Journal of Electrical and Electronics Engineering*, 2009, pp. 520–532.
- [16] F. Shiqing, D. Franitza, T. Marc, B. Frank, and M. Hiller, "Motion control of a tendon-based parallel manipulator using optimal tension distribution," in *IEEE/ASME Transactions On Mechatronics*, vol. 9, 2004, pp. 561–568.
- [17] M. A. Khosravi and H. D. Taghirad, "Experimental performance of robust PID controller on a planar cable robot," in *Mechanisms and Machine Science*. Springer Berlin Heidelberg, 2013, pp. 337–352.
- [18] B. Zi, B. Duan, J. Du, and H. Bao, "Dynamic modeling and active control of a cable-suspended parallel robot," *Mechatronics*, vol. 18, no. 1, pp. 1–12, 2008.
- [19] L. Jian, T. Xiaoqiang, S. Zhufeng, and Y. Rui, "Hybrid position/force control strategy and experiment of a six-cable driven parallel manipulator for a forty-meter aperture radio telescope," in *High Technology Letters*, 2012.
- [20] S. K. Agrawal and A. B. Alp, "Cable suspended robots: feedback controllers with positive inputs," in *American Control Conference, 2002. Proceedings of the 2002*, vol. 1, 2002, pp. 815–820.
- [21] W. Kraus, P. Miermeister, and A. Pott, "Investigation of the Influence of Elastic Cables on the Force Distribution of a Parallel Cable-Driven Robot," in *Mechanisms and Machine Science*, T. Bruckmann and A. Pott, Eds. Springer Berlin Heidelberg, 2013, pp. 103–115.
- [22] A. Pott, "Influence of pulley kinematics on cable-driven parallel robots," in *Latest Advances in Robot Kinematics*, J. Lenarcic and M. Husty, Eds. Springer Netherlands, 2012, pp. 197–204.
- [23] A. Pott, T. Bruckmann, and L. Mikelsons, "Closed-form force distribution for parallel wire robots," in *Proceedings of 5th International Workshop on Computational Kinematics 2009, May 6-8*. Duisburg, Germany: Springer-Verlag, 2009, pp. 25–34.
- [24] W. Kraus, V. Schmidt, P. Rajendra, and A. Pott, "Load identification and compensation for a cable-driven parallel robot," in *International Conference on Robotics and Automation (ICRA)*, May 2013.